Identification of Novel *FZD4* Mutations in Familial Exudative Vitreoretinopathy and Investigating the Pathogenic Mechanisms of *FZD4* Mutations

Erkuan Dai,[1] Min Liu,[2,3] Shujin Li,[2,3] Xiang Zhang,[1] Shiyuan Wang,[1] Rulian Zhao,[2,3] Yunqi He,[2,3] Li Peng,[2,3] Liting Lv,[2,3] Haodong Xiao,[1] Mu Yang,[2,3] Zhenglin Yang,[2,3] and Peiquan Zhao[1]

[1]Department of Ophthalmology, Xin Hua Hospital Affiliated to Shanghai Jiao Tong University School of Medicine, Shanghai, China
[2]Sichuan Provincial Key Laboratory for Human Disease Gene Study, Center for Medical Genetics and Department of Laboratory Medicine, Sichuan Provincial People's Hospital, University of Electronic Science and Technology of China, Chengdu, China
[3]Research Unit for Blindness Prevention, Chinese Academy of Medical Sciences (2019RU026), Sichuan Provincial People's Hospital, Chengdu, Sichuan, China

Correspondence: Peiquan Zhao, Department of Ophthalmology, Xin Hua Hospital Affiliated to Shanghai Jiao Tong University School of Medicine, Shanghai 200092, China; zhaopeiquan@126.com.
Zhenglin Yang, Sichuan Provincial People's Hospital, Chengdu, Sichuan 610072, China; yangzhenglin@cashq.ac.cn.
Mu Yang, Sichuan Provincial People's Hospital, Chengdu, Sichuan 610072, China; yang_mu@uestc.edu.cn.

ED, ML, and SL contributed equally to this work.

Received: January 22, 2024
Accepted: March 12, 2024
Published: April 1, 2024

Citation: Dai E, Liu M, Li S, et al. Identification of novel *FZD4* mutations in familial exudative vitreoretinopathy and investigating the pathogenic mechanisms of *FZD4* mutations. *Invest Ophthalmol Vis Sci*. 2024;65(4):1. https://doi.org/10.1167/iovs.65.4.1

Purpose. The purpose of this study is to report five novel *FZD4* mutations identified in familial exudative vitreoretinopathy (FEVR) and to analyze and summarize the pathogenic mechanisms of 34 of 96 reported missense mutations in *FZD4*.

Methods. Five probands diagnosed with FEVR and their family members were enrolled in the study. Ocular examinations and targeted gene panel sequencing were conducted on all participants. Plasmids, each carrying 29 previously reported *FZD4* missense mutations and five novel mutations, were constructed based on the selection of mutations from each domain of FZD4. These plasmids were used to investigate the effects of mutations on protein expression levels, Norrin/β-catenin activation capacity, membrane localization, norrin binding ability, and DVL2 recruitment ability in HEK293T, HEK293STF, and HeLa cells.

Results. All five novel mutations (S91F, V103E, C145S, E160K, C377F) responsible for FEVR were found to compromise Norrin/β-catenin activation of FZD4 protein. After reviewing a total of 34 reported missense mutations, we categorized all mutations based on their functional changes: signal peptide mutations, cysteine mutations affecting disulfide bonds, extracellular domain mutations influencing norrin binding, transmembrane domain (TM) 1 and TM7 mutations impacting membrane localization, and intracellular domain mutations affecting DVL2 recruitment.

Conclusions. We expanded the spectrum of *FZD4* mutations relevant to FEVR and experimentally demonstrated that missense mutations in *FZD4* can be classified into five categories based on different functional changes.

Keywords: FEVR, FZD4, missense mutation, Norrin/β-catenin signaling

Familial exudative vitreoretinopathy (FEVR) is a hereditary eye disorder first identified by Criswick and Schepens[1] in 1969, characterized by aberrant vascular development in the retina. The hallmark pathological feature of FEVR is a delay in retinal vascular development, resulting in avascular zones in the peripheral retina, pathological neovascularization, hemorrhage, fibrovascular proliferation, and consequent retinal detachment, which often leads to blindness in childhood.[2] To date, research has identified 17 genes and one genetic locus implicated in FEVR.[3–19] Mutations in genes associated with the Norrin/β-catenin pathway, specifically *NDP*, *FZD4*, *LRP5*, *TSPAN12*, and *CTNNB1*, predominate in FEVR cases, with the other 11 genes all having no more than three reported cases of mutations. Two large-scale studies have shown the reported genes can explain nearly half of FEVR cases. *LRP5* contribute to approximately 37% and *FZD4* to 29% of the explainable FEVR cases, being the two genes with the highest proportions.[20,21]

The *FZD4* gene encodes a 537-amino acid protein with distinct functional domains, including an N-terminal cysteine-rich domain (CRD), seven transmembrane domains, and a C-terminal S/T-X-V motif. As a member of the Frizzled family of transmembrane receptors, FZD4 plays a crucial role in regulating the Wnt signaling pathway.[22] Studies using *Fzd4* knockout models have successfully replicated

the observed features of FEVR, mainly attributed to impaired Norrin/β-catenin signals. Restoration of these signals via β-catenin overexpression has been shown to reverse the conditions' features.[23]

After the identification of FEVR-associated mutations in the *FZD4* gene in 2002,[24] a global body of case reports involving *FZD4* mutations has emerged. Mutations in *FZD4* encompass a spectrum of types, including missense, frameshift, nonsense, insertion, deletion, copy number variation (CNV), and splicing. In a recent report based on a large population, the two most prevalent *FZD4* mutation types were found to be missense (45%) and deletion mutations (25.5%).[25] However, most reports are clinical case studies lacking detailed analysis of the mutations' specific functional implications. The following studies have shed some light on the functional changes of *FZD4* mutations in the Norrin/β-catenin signaling pathway. Smallwood et al.[26] identified the sequences in the CRD of FZD4 that binds to norrin through alanine scanning and block substitution. Additionally, studies have reported that Y58C and M105R mutations affect binding to norrin.[27,28] Furthermore, a series of mutations leading to defective trafficking of FZD4 have been found.[29] Finally, it has been reported that R253H and F328S reduce the ability of FZD4 to recruit DVL2,[30] and Y250 is also an important FZD-DVL interaction site.[31]

In this study, we identified five novel *FZD4* missense mutations in FEVR patients. Through a comprehensive review of reported mutations linked to FEVR, we conducted an in-depth analysis of a diverse array of missense mutations spread across the *FZD4* gene. Our focus was to unravel the distinct mechanisms of pathogenicity associated with mutations situated in various domains. We selected to analyze missense mutations because they alter single amino acids, allowing for a more precise examination of the functional roles of amino acids located within structural domains.

Material and Methods

Ethical Declarations, Clinical Evaluation, and Gene Sequencing

The study was approved by the institutional ethics committees of Xinhua Hospital Affiliated with Shanghai Jiao Tong University School of Medicine. All participants were recruited from this single instruction, and written informed consent was obtained either from each individual or from their legal guardian(s) in the case of minors.

Each proband underwent ocular examinations, including wide-field fundus photography using either a RetCam (Natus Medical Incorporated, Middleton, WI, USA) or an Optos 200Tx (Optos, Dunfermline, UK), as well as indirect ophthalmoscopy with a 28D lens and scleral depression when required. When eligible, the proband and their parents underwent fundus fluorescein angiography (FFA). The diagnosis of FEVR was based on the presence of at least one of the following retinal vascular developmental anomalies: a lack of peripheral retinal vasculature with or without nonperfusion, vitreoretinal traction, subretinal exudation, retinal neovascularization at any age, or total retinal detachment with a fibrotic mass behind the lens.[32] Patients with a history of premature birth were excluded. Targeted gene capture and sequencing procedures followed previously established protocols (MyGenostics), and Sanger sequencing was carried out to validate the variants as previously described.[21]

Cell Culture and Plasmids Construction

HEK293T cells, HEK293STF cells, and HeLa cells (American Type Culture Collection and Cell Systems) were cultured at 37°C in a humidified 5% CO_2 incubator in DMEM supplemented with 10% fetal bovine serum a 1% penicillin/streptomycin.

The human *FZD4* (NM_012193) coding sequence was subcloned into the pcDNA3.1 vector with a C-terminal HA tag. The mutations were introduced into the wild-type (WT) expression plasmid by site-directed mutagenesis with the Q5 Site-Directed Mutagenesis Kit (New England Biolabs, Ipswich, MA, USA). The *FZD5*, *LRP5, LRP6, NDP, DVL2* and pDsRed2-ER plasmids were obtained from Youbio Biotechnology (Changsha, China). The *FZD5* plasmid has a C-terminal HA tag, the *NDP* plasmid has a C-terminal Myc-FLAG tag, and the *DVL2* plasmid has a C-terminal FLAG tag. The pGL4.1-*Renilla* was sourced from Promega (Madison, WI, USA). Plasmids were transfected by EntransterTM-H4000 transfection reagent (Engreen Biosystem Co, Ltd, Auckland, New Zealand).

Western Blot and Co-Immunoprecipitation (Co-IP)

HEK293T cells were seeded into six-well plates and transfected with 1200 ng WT FZD4 or mutant plasmids. After 48 hours, total cell protein was extracted on ice with lysis buffer (150 mM NaCl, 50 mM Tris-HCl pH 8.0, 1% Triton X-100) in the presence of protease inhibitor cocktail. Cell lysates were mixed with 5 × loading buffer and then heated at 37°C for 30 minutes. For detection of glycosylation, protein samples were treated with EndoH (New England Biolabs) or PNGaseF (Yeasen, Shanghai, China) according to the manufacturer's instructions.

For generation of norrin-conditioned medium, HEK293T cells were cultured in 10 cm dish and transfected with 10,000 ng NDP-Myc-FLAG plasmid. After 72 hours, the culture medium was collected and spun in a centrifuge at 900*g* for three minutes, after which the supernatant was transferred into new tubes. For Co-IP, after incubation of norrin conditioned medium for 45 minutes at 4°C, cells were washed three times with ice-cold PBS and lysed. Cell lysates were spun in a centrifuge for 15 minutes at 13,000 *g* at 4°C and 10% of the supernatants were collected into new tubes for input. The rest of soluble supernatants were rotated with anti-HA-magnetic beads at room temperature for two hours. After four washes with lysis buffer, the samples were resuspended in loading buffer and heated at 37°C for 30 minutes. The beads were discarded, and the supernatants were used for Western blotting. The following antibodies were used for immunoblots: rabbit anti-FLAG (20543-1-AP; Proteintech, Rosemont, IL, USA), rat anti-HA (3F10; Roche, Basel, Switzerland), rabbit anti-GAPDH (10494-1-AP; Proteintech), anti-rabbit and anti-rat secondary antibody conjugated with horseradish peroxidase (SA0001-2 and SA00001-15; Proteintech).

RT-qPCR

Total RNA was extracted from HEK293T cells transfected with WT, mutant, or vector plasmids using TrizolUP (TransGen Biotech, Beijing, China). Subsequently, 1 µg of total RNA was reverse-transcripted into cDNA with TranScript All-in-one First-Strand cDNA Synthesis Super-

Mix (TransGen Biotech). The cDNA was then amplified and detected with the 7500 Fast Real-Time PCR System (Applied Biosystems, Foster City, CA, USA). The fold changes of FZD4 were normalized to GAPDH. Primers: *GAPDH* (Forward: 5′- CTGACTTCAACAGCGACACC-3′ and Reverse: 5′- TGCTGTAGCCAAATTCGTTG-3′) and *FZD4* (Forward: 5′- GTCTCAGTCTGGGGTTGCTC-3′ and Reverse: 5′- GTCACGTTGTAGCCGAGGTT-3′).

Immunofluorescence Staining

After transfection with the corresponding plasmids, cells cultured on poly-l-lysine–coated coverslips were first washed twice with PBS and then fixed with 4% PFA (BioSharp, Tallinn, Estonia) at room temperature for 15 minutes. To label the cell membrane, cells were incubated with Wheat Germ Agglutinin (WGA)-647 (W32466; ThermoFisher, St. Louis, MO, USA) for 10 minutes before fixation. To analyze the norrin-binding ability of FZD4 mutants, cells were incubated at 4°C in norrin-conditioned medium for 45 minutes before fixation, followed by three washes with ice-cold PBS. After fixation, the coverslips underwent three washes with PBS and were subsequently blocked using a buffer (5% FBS and 0.2% Triton X-100 in PBS) for one hour. Next, the coverslips were incubated with primary antibodies diluted in blocking buffer overnight at 4°C. On the next day, the coverslips were washed with PBS three times and then incubated with fluorescently labeled secondary antibodies and DAPI (4083; Cell Signaling Technology, Danvers, MA, USA) for one hour at room temperature. Fluorescence was observed using an LSM900 confocal microscope (Zeiss, Oberkochen, Germany) equipped with a 63 × oil-immersion objective. Colocalization analysis was performed using the Pearson correlation coefficient method in Fiji.

To evaluate the norrin-binding affinity of FZD4 mutants accurately, the fluorescence intensity of FZD4 was standardized during cell selection to maintain consistency in FZD4 expression levels across the analyzed cells. We identified notable variances in FZD4 fluorescence intensity on individual cell membranes. To mitigate this variability, we selected regions with moderate fluorescence intensity, marking a 1 µm line segment and measuring FZD4 and NDP fluorescence intensity at that location. The fluorescence values along the line segment were averaged, and then the relative strength of NDP was calculated by dividing NDP's fluorescence intensity by FZD4's fluorescence intensity. The following antibodies were used for immunofluorescence: rat anti-HA (3F10; Roche), rabbit anti-FLAG (14793S; Cell Signaling Technology), Alexa fluor 488 donkey anti-rat (A-21208; ThermoFisher), Alexa fluor 647 donkey anti-rabbit (A-31573; ThermoFisher).

Dual-Luciferase Reporter Assay

To assess the Norrin/β-catenin activation capacity of the FZD4 mutants, HEK293STF cells were transfected with 100 ng pGL4.1-Renilla, 25ng LRP5, and increasing amounts of WT FZD4, mutant FZD4, or vector plasmid (5 ng, 15 ng, and 25 ng). After 24 hours, the cells were incubated in norrin-conditioned medium for another 24 hours. To assess the canonical WNT pathway activation capacity of the FZD4 mutants in the absence of a ligand, HEK293STF cells were transfected with 100 ng pGL4.1-Renilla, 50 ng LRP6, and 50 ng WT FZD4, mutant FZD4, or vector plasmid and incubated for 48 hours. The transfected cells were then subjected to luciferase activity assays using the Dual-Luciferase Reporter Assay System (Yeasen) according to the manufacturer's protocols. Reporter activity was calculated as the ratio of firefly luciferase activity to Renilla luciferase activity.

Statistical Analysis

Data were expressed as mean ± SD. One-way ANOVA were used. All statistical evaluations and graphs were generated in GraphPad Prism 8.0 software. Statistical significance was set at $P < 0.05$.

Results

Identification of Five Novel *FZD4* Missense Mutations in FEVR patients

Five novel *FZD4* mutations were identified in FEVR patients diagnosed at Xinhua hospital, all of which were predicted as pathogenic through in silico analysis (Table 1). Further validation of these mutations was conducted using Sanger sequencing, for which all exhibited genotype-phenotype cosegregation (Fig. 1A). The fundus of all probands manifested typical FEVR phenotypes, including peripheral avascular area or retinal folds (Figs. 1B–F). Consistent with previous reports,[33,34] we found that clinically affected father or mother within the same family exhibited milder phenotypes, mostly manifesting only peripheral supernumerary branching or avascular areas on FFA (Fig. 1G).

Assessment of Mutations in Different Domains of FZD4 on Protein Expression and Norrin/β-catenin Signaling Activity

In order to investigate the pathogenic mechanisms of five novel mutations, we conducted a comprehensive literature review up to June 2023 using a search on PubMed with keywords "FZD4 and FEVR," gathering all documented

Table 1. Novel *FZD4* Mutations Found in This Study

No	Nucleotide Change	Protein Change	1000G	ExAC	PolyPhen-2	PhyloP100	CADD	REVEL	Heredity	Cosegregation	ACMG
1	c.272C>T	p.S91F	0	0	0.982	1.506	29.8	0.698	Father	Yes	PS3
2	c.308T>A	p.V103E	0	0	0.999	4.471	28.7	0.667	Mother	Yes	PS3
3	c.433T>A	p.C145S	0	0	1.000	9.231	28.7	0.955	Father	Yes	PS3
4	c.478G>A	p.E160K	0	0	0.701	7.816	25.7	0.575	Father	Yes	PS3
5	c.1130G>T	p.C377F	0	0	1.000	7.767	29.8	0.925	Mother	Yes	PS3

In silico analyses used: PolyPhen-2 (http://genetics.bwh.harvard.edu/pph2/; provided in the public domain by Harvard University, Cambridge, MA, USA), PHRED- like Scaled CADD Score (https://cadd.gs.washington.edu/snv) and REVEL (https://sites.google.com/site/revelgenomics/). Refer to this literature for ACMG variant classification.[46]

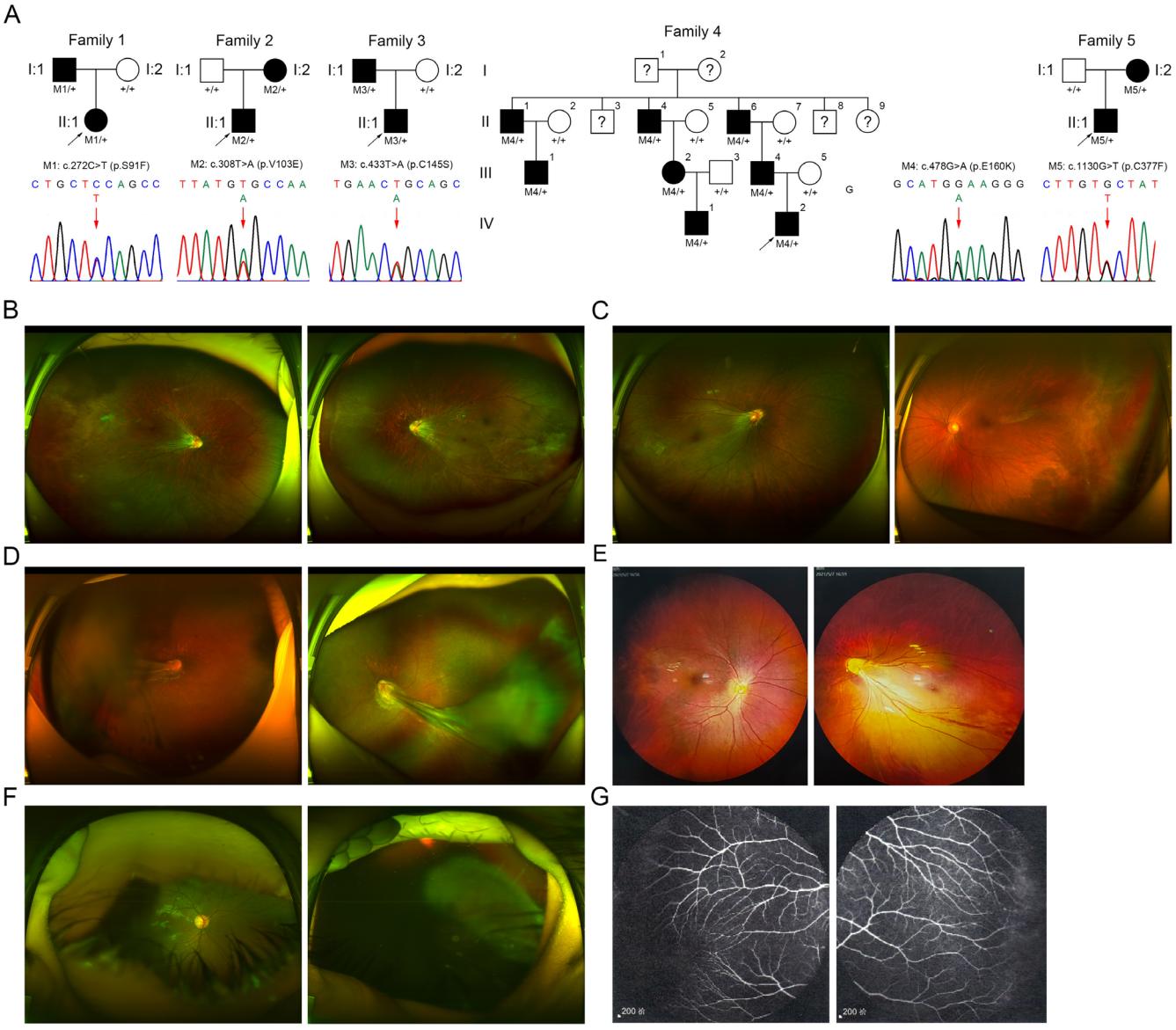

Figure 1. The pedigrees of the families with mutations in *FZD4* and the fundus images of probands and family members. (**A**) FEVR pedigrees and Sanger sequencing analysis of five FEVR-associated families. Affected individuals are represented in black, with the proband of each family indicated by a black arrow. The altered nucleotides are denoted by *red arrows*. (**B**) Fundus images of the proband in family 1 showing bilateral dragged discs. (**C**) Fundus images of the proband in family 2 showing dragged disc and temporal peripheral exudation in right eye and peripheral avascular area. (**D**) Fundus images of the proband in family 3 showing bilateral retinal folds. (**E**) Fundus images of the proband in family 4 showing dragged disc in left eye. (**F**) Fundus images of the proband in family 5. Because of retinal detachment, the left eye is not amenable to visualization. (**G**) FFA of the mother in family 5 showing supernumerary branching.

missense mutations. *FZD4* variants previously classified as benign in the literature were excluded from our analysis. From this review, we identified a total of 96 reported *FZD4* missense mutations in FEVR patients and classifying them by structural domains based on the reported crystal structure of the Norrin-Fz4$_{CRD}$ complex and FZD4 in the ligand-free state (Figs. 2A, 2B, Table 2).[35,36] The four mutations S91F, V103E, C145S, and E160K are located in the extracellular domain (ECD), which contains three loops that come into contact with norrin (Fig. 2B). Notably, novel mutations at positions 91 and 103 are located between loop I and loop II, and 145 is located between loop II and loop III. No previous analysis on whether mutations located between the loops can also affect norrin binding currently exists.

Additionally, *FZD4* mutations have been primarily reported in clinical case studies, lacking systematic analyses of their potential effects across various domains. To understand the impact of mutations at various domains within FZD4, we generated a total of 34 mutants selected distributed across the gene, encompassing 5 novel mutants reported in this study (Table 2). First, we assessed the impact of these mutations on protein expression in HEK293T cells. Under equivalent RNA expression levels (Supplementary Fig. S1), mutants at positions 145, 204, 223, 226, 228, 234, 377, and 488 exhibited significantly reduced protein expression levels (Fig. 2C, Supplementary Fig. S2). Furthermore, they showed decreased molecular weights which were later confirmed to be caused by lack of post-translational modifications (Fig. 3A). Given that there is only one *FZD4* transcript in humans, the presence of multiple bands for Y58C, V103E, I114S, W139S, and M157T suggests the potential occurrence of distinct modifications (Fig. 2C). Subsequently,

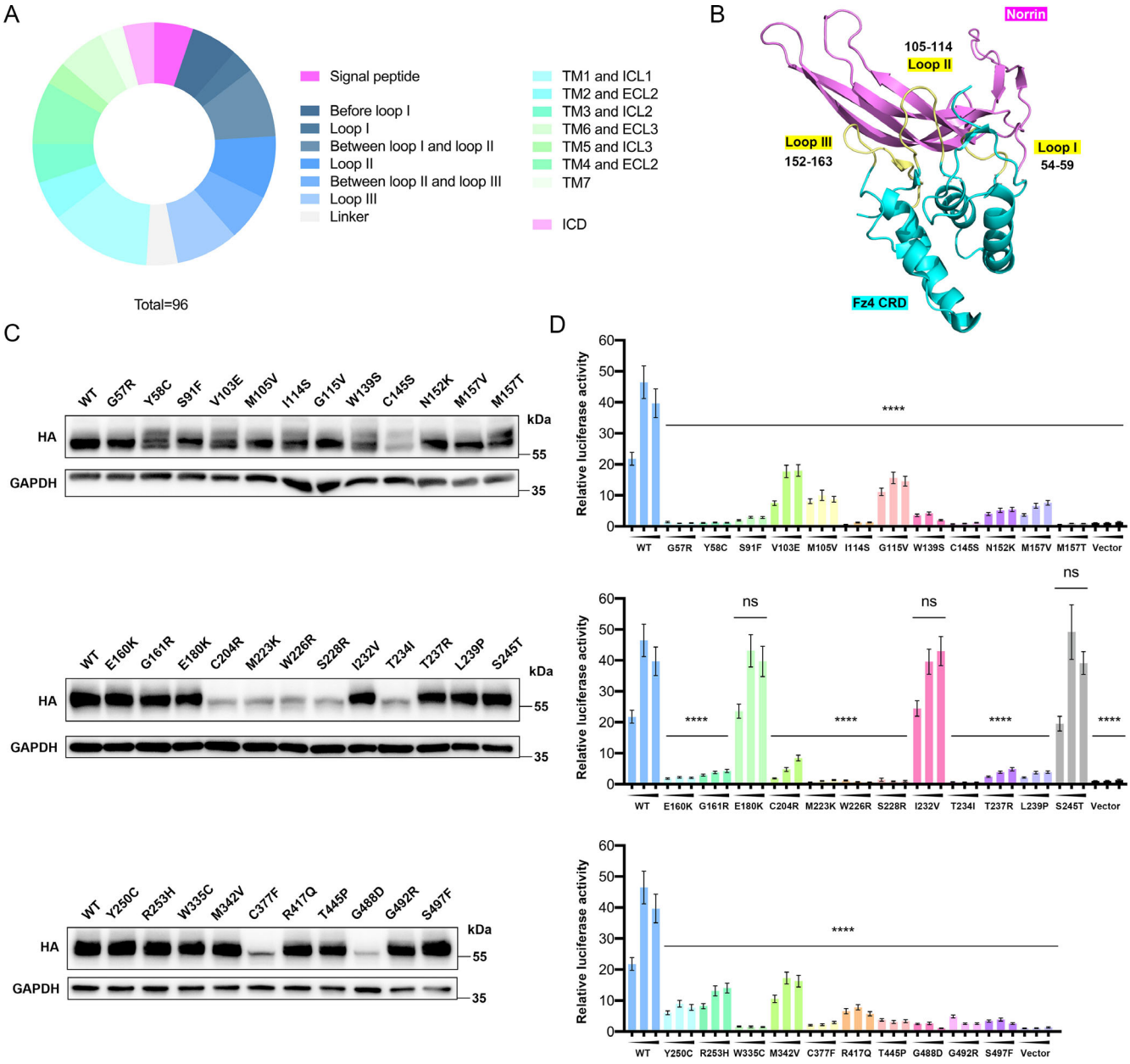

Figure 2. Classification of all reported missense mutations in *FZD4* in FEVR patients and assessment of expression levels and Norrin/β-catenin signaling activity of 34 mutations. (**A**) Classification of FZD4 functional domains and disease-associated mutations. ICL, intracellular loop; ECL, extracellular loop; ICD, intracellular domain. (**B**) Lateral depiction of the Norrin-Fz4$_{CRD}$ complex, with coloring denoted as *blue* (Fz4$_{CRD}$), *yellow* (loop I-III), and *pink* (Norrin) (PDB ID = 5BQC). (**C**) Western blot of HA-tagged FZD4 protein level in HEK293T cells transfected with WT or mutants. (**D**) Relative STF luciferase activity after transfecting increasing dosage of WT or mutant FZD4 (5 ng, 15 ng, and 25 ng) together with LRP5 into HEK293STF cells, followed by incubation with norrin conditioned medium. Normalization was performed based on the values from the 5 ng dose of the vector group (n = 3). *Error bars*: SD. One-way ANOVA with Dunnett's multiple comparisons test was performed to compare each mutant and WT within each dosage group. ****$P < 0.0001$; ns, not significant.

using luciferase assays to evaluate the ability of these FZD4 mutants to activate Norrin/β-catenin signaling, we found that, with the exception of E180K, I232V, and S245T, which showed no significant differences compared to the wild-type, all other mutations compromised the activation ability (Fig. 2D). E180K, I232V, and S245T exhibited similar behavior to WT in all subsequent experiments. Further literature review revealed that these mutations lack explicit hereditary information and in silico analysis indicated low likelihood of pathogenicity, suggesting they are more likely benign variants rather than mutations (Supplementary Table S1).

Analysis of Membrane Localization of FZD4 Mutants

To investigate the mechanisms underlying decreased activation of the Norrin/β-catenin pathway due to *FZD4* mutations, we initially examined their impact on membrane localization, which is prerequisite for the functional role of FZD4 as a receptor. We used selective enzymes (EndoH and PNGaseF) to evaluate the cell surface proportion and immature form of FZD4 before Golgi processing.[37] Mature glycoproteins passing through the Golgi apparatus exhibit

Table 2. All Missense Mutations of *FZD4* in FEVR Patients

Domain and Amino Acid Positions	Protein Change	Wnt Activity	Membrane Localization	Norrin Binding	DVL2 Recruitment	Reference
Signal peptide (1-36)						
	P11E					47
	G22E					48
	P33S		Affected			29
	G36D					49
	G36N		Affected			29
Before loop I (37-53)						
	E40Q					50
	C45R					51
	C45S					51
	C45Y	Decreased	Affected	Affected		27
	S51T					43
	C53S					51
Loop I (54-59)						
	G57C					43
	G57R*					25
	Y58C*	Decreased	N.C.	Affected		27
Between loop I and loop II (60-104)						
	T61I					21
	H69Y		Affected			29
	A75T					51
	A75G					21
	C90R					51
	S91F*					This study
	Q95L					52
	C99S	Increased	N.C.			53
	V103E*					This study
Loop II (105-114)						
	M105V*		N.C./Affected	N.C.		29, 44
	M105R	Decreased		Affected		28
	M105T		Affected			29
	C106G					54
	C106S					21
	I114T					55
	I114S*					56
	I114N					21
Between loop II and loop III (115-151)						
	G115V*	Decreased				57
	C117R	Decreased				43
	C117W					25
	C128R					21
	W139S*					47
	C145S*					This study
Loop III (152-163)						
	N152K*					58
	H154R					59
	M157V*	Decreased	N.C.	N.C.		44
	M157T*					60
	M157K					54
	E160Q					21
	E160K*					This study
	G161R*					47
Linker (164-203)						
	P168S					49
	E180K*	Decreased		N.C.		40
	C181R		Affected			29
	C181Y					29
TM1 and ICL1 (204-249)						
	C204R*	Decreased	Affected	Affected		29
	C204Y		Affected			29
	C204F					61

Table 2. Continued

Domain and Amino Acid Positions	Protein Change	Wnt Activity	Membrane Localization	Norrin Binding	DVL2 Recruitment	Reference
	Y211H	Decreased	N.C.			62
	M223K*					63
	W226R*					60
	S228R*					41
	L229P					64
	I232V*					41
	T234I*					21
	T237R*	Decreased	N.C.			30
	L239P*					65
	S245T*					41
TM2 and ECL1 (250-299)						
	Y250C*					66
	R253H*	Decreased	N.C.		Affected	30
	L273R					67
	I293V					41
	K298E					68
TM3 and ICL2 (300-336)						
	C302Y	Decreased				69
	I322F					70
	L325R					25
	F328S	Decreased	N.C.		Affected	30
	W335C*		N.C.			29
TM4 and ECL2 (337-383)						
	A339T					48
	M342V*					71
	S344R					41
	S344T					41
	F347V		N.C.			72
	H348Q					58
	K358N					43
	C377F*					This study
TM5 and ICL3 (384-431)						
	P394L					25
	R417Q*	Decreased	N.C.	N.C.		73
	L420I					59
TM6 and ECL3 (432-473)						
	M434V					41
	I437T	Decreased				57
	V442E	Decreased				69
	L443P					64
	T445P*		N.C.			29
	D470N	N.C.	N.C.			48
TM7 (474-495)						
	G488D*		Affected			29
	G488V					54
	G492R*		N.C.			29
ICD (496-537)						
	S497F*					16
	L501P					41
	G525R					50
	G530E					43

ICL, intracellular loop; ECL, extracellular loop; ICD, intracellular domain; N.C., no change.
* The mutations investigated in this study.

complex N-glycans, while high-mannose type glycans are primarily displayed in the endoplasmic reticulum (ER). Treatment with EndoH distinguishes between these types, as it cleaves high-mannose and hybrid glycans but not complex N-glycans. Compared to the wild type, the proportion of C145S, C204R, M223K, W226R, S228R, T234I, C377F, and G488D mutants resistant to EndoH was significantly reduced (Figs. 3A, 3C), whereas the other mutations showed no significant differences (Supplementary Fig. S3). Furthermore, the expression levels of these mutants were also affected (Supplementary Fig. S2), implying potential degradation by the ER quality control system. Through overexpressing mutant FZD4 and DsRed2-ER plasmid in HeLa cells and using WGA staining for cell membrane labeling, we

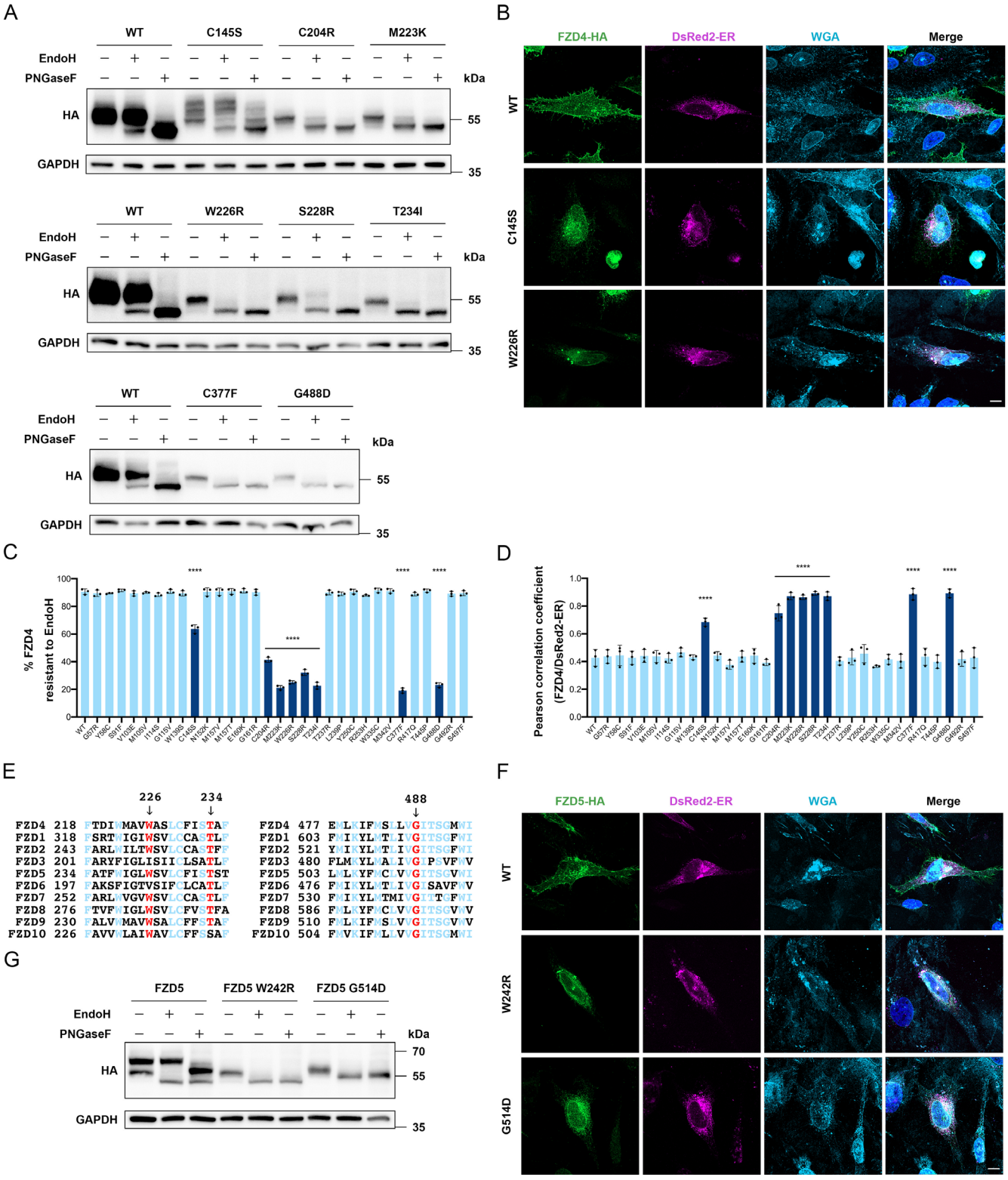

Figure 3. Membrane localization analysis of FZD4 Mutants. (**A**) Western blot analysis of Endo H or PNGaseF treated cell lysates of HEK293T cells transfected with WT or mutant FZD4. (**B**) Representative immunofluorescence images of FZD4 (*green*), ER (*magenta*), WGA (*light blue*), DAPI (*blue*) in HeLa cells transfected with FZD4 (WT or mutants) and pDsRed2-ER. *Scale bar*:10 µm. (**C**) Densitometry analysis of Endo H resistant proportion of WT or mutant FZD4 protein expressed in HEK293T cells (n = 3). *Error bars*: SD. (**D**) Co-localization analysis using the Pearson correlation coefficient (n = 20). *Error bars*: SD. (**E**) Alignment of all human Frizzled receptor homologs based on the amino acids at position 226 and 488 of FZD4. (**F**) Immunofluorescence images of FZD5 (*green*), ER (*magenta*), WGA (*light blue*), DAPI (*blue*) in HeLa cells transfected with FZD5 (WT or mutants) and pDsRed2-ER. *Scale bar*:10 µm. (**G**) Western blot analysis of Endo H or PNGaseF treated cell lysates of HEK293T cells transfected with WT or mutant FZD5. One-way ANOVA with Dunnett's multiple comparisons test was performed to compare each mutant and WT for **C** and **D**. ****$P < 0.0001$.

Investigative Ophthalmology & Visual Science

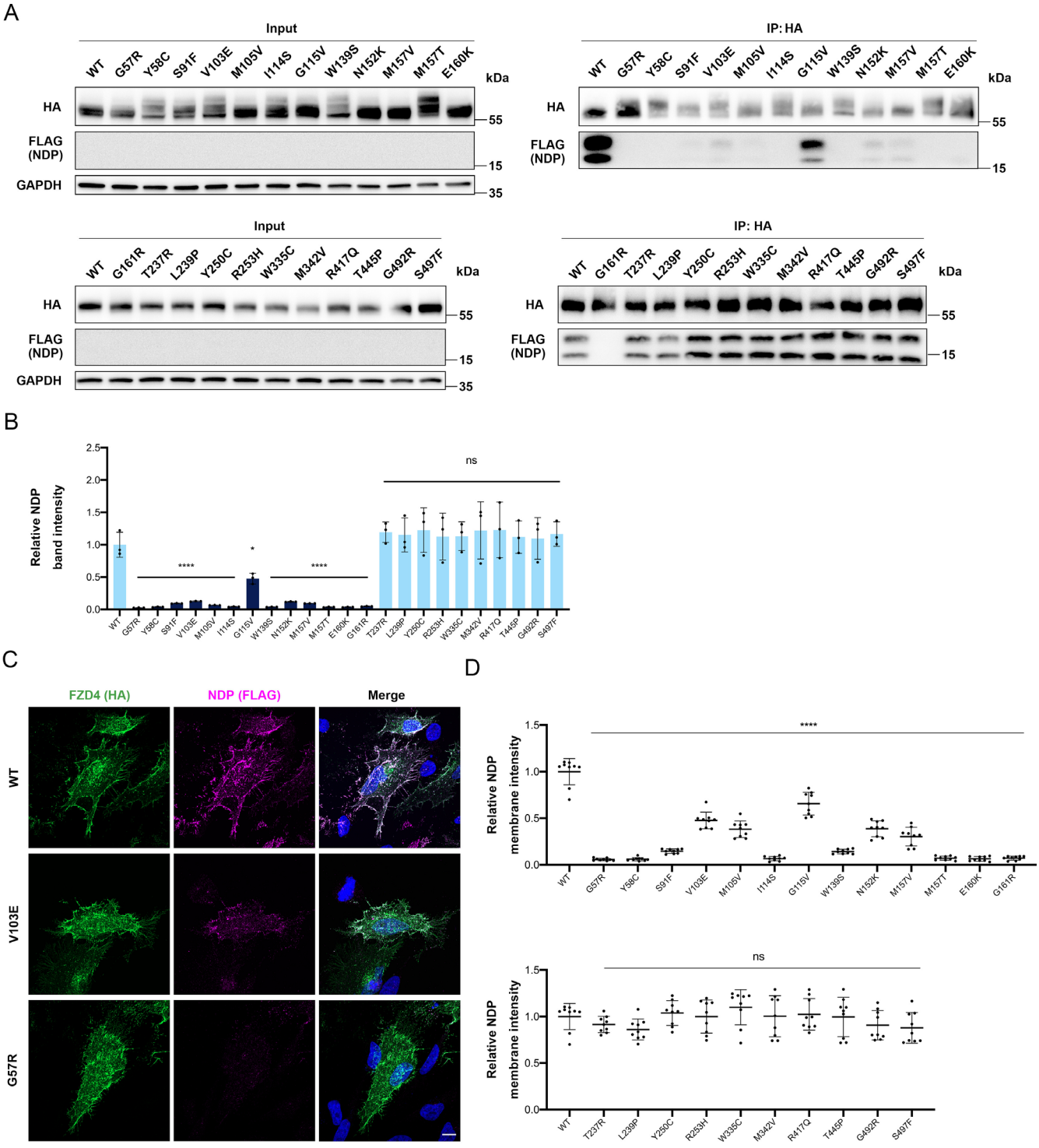

Figure 4. Norrin binding analysis of FZD4 Mutants. (**A**) Western blot analysis of norrin conditioned medium co-immunoprecipitated with FZD4-HA (WT or mutants). Because of the 1:9 ratio of input to IP, the quantity of norrin in the input is insufficient to be detected. (**B**) The NDP band intensity in the immunoprecipitation was normalized to the pulldown HA (FZD4) band, and further standardized for each mutant relative to WT values (n = 3). *Error bars*: SD. (**C**) Representative immunofluorescence images of FZD4 (*green*), NDP (*magenta*), and DAPI (*blue*) in HeLa cells transfected with FZD4-HA (WT or mutants) and incubated with norrin conditioned medium. *Scale bars*: 10 µm. (**D**) Quantification of membrane signal intensity of NDP in HeLa cells transfected with FZD4-HA (WT or mutants) and incubated with norrin conditioned medium (n = 10). *Error bars*: SD. Experiments were performed independently at least three times. Normalization was performed against the WT. One-way ANOVA with Dunnett's multiple comparisons test was performed to compare each mutant and WT for **B** and **D**. *$P < 0.05$; ****$P < 0.0001$; ns, not significant.

Investigative Ophthalmology & Visual Science

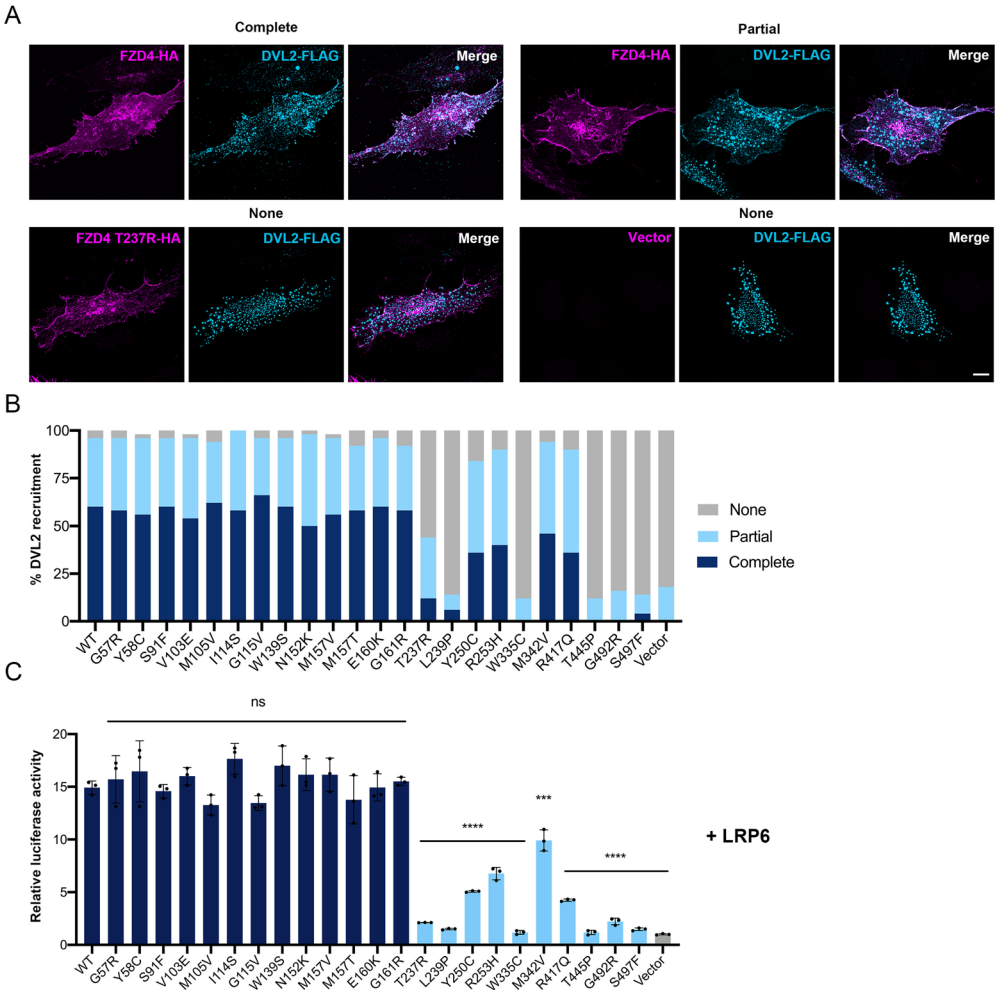

Figure 5. DVL2 recruitment analysis of FZD4 Mutants. (**A**) Representative immunofluorescence images of FZD4 (*magenta*) and DVL2 (*light blue*) in HeLa cells transfected with FZD4-HA (WT, mutants or vector). *Scale bar*:10 µm. (**B**) Quantification of DVL2 recruitment to the membrane by WT FZD4 and mutants (n = 50). (**C**) Relative STF luciferase activity after transfecting WT or mutant FZD4 or vector with LRP6 into HEK293STF cells. Normalization was performed based on the values of the vector group (n = 3). *Error bars*: SD. One-way ANOVA with Dunnett's multiple comparisons test was performed to compare each mutant or vector and WT. ***$P < 0.001$; ****$P < 0.0001$.

observed that C145S, C204R, M223K, W226R, S228R, T234I, C377F, and G488D exhibited reduced membrane localization and enhanced co-localization with ER, whereas the other mutations did not show significant differences compared to WT (Figs. 3B, 3D, Supplementary Fig. S4).

C145S, C204R, and C377F occur at positions crucial for the formation of intramolecular disulfide bonds, and substitutions of cysteine at these sites may exert an influence on the proper protein folding. M223K, W226R, S228R, T234I are all located with TM1, whereas G488D is located with TM7. Notably, our sequence alignment analysis revealed a relatively high degree of conservation for the amino acids tryptophan (W) at position 226, threonine (T) at position 234, and glycine (G) at position 488 of FZD4 among human Frizzled receptor homologs (Fig. 3E). We were curious whether mutations at these specific positions might also affect the membrane localization of other Frizzled receptors. Therefore we generated corresponding mutations in human *FZD5*, specifically FZD5 W242R corresponding to FZD4 W226R, and FZD5 G514D corresponding to FZD4 G488D. Our subsequent EndoH analysis and immunofluorescence staining unequivocally revealed that these two mutations also led to a significantly impaired localization of FZD5 to the membrane (Figs. 3F, 3G), indicating the significance of these positions for the maturation of Frizzled receptors.

Analysis of Binding Capability to Norrin of FZD4 Mutants

After excluding mutations that affect expression and membrane localization, we further explored the pathogenic mechanisms of the remaining mutations. The CRD domain of FZD4 is essential for norrin binding,[26,27] and we aimed to confirm whether each mutation in ECD would lead to weakened norrin binding and whether mutations outside the ECD could also affect norrin binding. By overexpressing WT FZD4 or mutant forms in HEK293T cells incubated with norrin conditioned medium, we conducted Co-IP experiments to analyze the ability of FZD4 to bind norrin in the supernatant (Fig. 4A). G115V showed a mild reduction in norrin binding, while G57R, Y58C, S91F, V103E, M105V, I114S, W139S, N152K, M157V, M157T, E160K, and G161R displayed severe reductions in binding capacity (Fig. 4B). Mutations in domains outside the ECD exhibited norrin binding capacities similar to WT. Additionally,

through immunofluorescence staining, we quantified the amount of membrane-bound norrin in HeLa cells overexpressing WT FZD4 or mutants after incubation of norrin conditioned medium (Figs. 4C, 4D, Supplementary Fig. S5), with results consistent with the Co-IP findings. The degree of reduction in norrin binding ability because of mutations in ECD corresponds closely to the impairment of the ability to activate the Norrin/β-catenin signaling pathway.

Analysis of DVL2 Recruitment of FZD4 Mutants

Previous studies have indicated that the activation of the canonical β-catenin pathway requires FZD-mediated recruitment of DVL2,[38] with all intracellular domains of FZD being essential for FZD-DVL interaction.[39] In the case of FZD4, the R253H and F328S mutations have been found to impact the recruitment of DVL2,[30] and another study has highlighted the significance of the Y250 to recruit DVL2.[31] This prompted us to investigate whether mutations in *FZD4*, previously shown to reach the membrane and bind norrin normally, could impact DVL2 recruitment. Overexpression of DVL2-FLAG and vector in HeLa cells resulted in punctate distribution within the cells (Fig. 5A). However, coexpression with wild-type FZD4 led to complete recruitment of DVL2 to the cellular membrane in 60% of the transfected cells, whereas partial recruitment to the membrane was observed in 36% of the transfected cells, retaining the punctate intracellular pattern (Fig. 5A). The mutations Y250C, R253H, M342V, and R417Q exhibited significantly reduced DVL2 recruitment, whereas T237R, L239P, W335C, T445P, G492R, and S497F almost entirely lost their ability to recruit DVL2. In contrast, mutations located in the ECD still retained recruitment abilities comparable to the wild type (Fig. 5B). To validate these findings, we explored the overexpression of FZD4 and LRP6 to evaluate the capacity of FZD4 mutants to activate the WNT/β-catenin signaling pathway in the absence of ligands like Norrin or WNT. As anticipated, FZD4 mutants incapable of effectively recruiting DVL2 displayed markedly diminished WNT signaling pathway activation through LRP6 (Fig. 5C).

Discussion

Pathogenicity Assessment of Variants

Upon scrutinizing all examined mutations, E180K, I232V, and S245T exhibited no significant deviations from WT in all assays. Upon literature review, we noted the absence of family information for these mutations in the original reports.[40,41] Use of in silico analyses, such as PolyPhen-2 and REVEL, indicated that these three mutations lean toward benign variants. Hence, we recommend reclassifying these three mutations as benign variants. In contrast, the five newly reported mutations S91F, p.V103E, C145S, E160K, and C377F all have available family information, are in line with genotype-phenotype cosegregation and are predicted as pathogenic by multiple prediction programs. This underscores the pivotal role of family history in evaluating the pathogenicity of newly identified variants. The predictions from PolyPhen-2 and REVEL closely match up with our wet laboratory experiments and can serve as a basis for assessing the pathogenicity of variants.

Phenotypic variability is frequently observed in FEVR.[25,33] The five novel mutations identified in this study also align with the trend where probands exhibit more severe phenotypes than their family members. Notably, on individual proband phenotype analysis, patients with mutations affecting FZD4 protein expression, such as C145S and C377F, displayed more severe phenotypes compared to those with mutations (S91F, V103E, and E160K) that solely impact norrin binding without affecting protein expression. We speculate that mutations causing more pronounced protein functional impairment pose a higher risk of developing severe phenotypes.

Importance of the ECD of FZD4 in Norrin Binding

The CRD domain is the primary domain in the extracellular region of FZD4 responsible for norrin binding, spanning from amino acid 45 to 158. Previous studies have identified certain regions within the CRD, including 55–60, 105–107, 125–130, 133–137, and 151–157, for norrin binding through rigorous and comprehensive substitution experiments.[26] The crystal structure of the Norrin-Fz4$_{CRD}$ complex has unveiled three loops directly binding to norrin,[35] substantiating findings from earlier biochemical experiments. It is conceivable that mutations occurring in the crucial norrin-binding regions mentioned above are likely to lead to weakened norrin binding. In this study, we experimentally verified the importance of these regions and intriguingly discovered that mutations in the amino acids connecting these critical regions may also compromise norrin binding, such as S91F, V103E, G115V, and W139S. Notably, even a slight weakening of the interaction between FZD4 and norrin, as seen with G115V, is sufficient to cause approximately a 50% reduction in Norrin/β-catenin signaling activity, which can lead to the development of FEVR.

Previous studies have underscored the importance of the FZD4 linker (between loop III and TM1, amino acids 164-203) in norrin binding and the essential role of the FZD6 linker domain in receptor localization.[40,42] Encountering only four reported linker mutations in FEVR, with two involving cysteine residues (C181R and C181Y), we assessed E180K and propose it to be a benign variant. Research indicated that the simultaneous presence of P168S and P33S result in a modest decline in Wnt activity.[43] This suggests that P168S may not affect the membrane localization of FZD4 but instead exerts an impact on norrin binding.

Classification of *FZD4* Missense Mutations

In summary of the above findings, we mapped mutations investigated in this study onto the full-length FZD4 amino acid sequence (Fig. 6). Classifying mutations that result in similar functional changes together, the following categories can be delineated: (1) Mutations in the signal peptide are generally predicted to affect protein maturation and trafficking. (2) Mutations involving cysteine residues forming intramolecular disulfide bonds, such as previously reported C45Y, C117R, C181R, C204R, C302Y, and newly identified C145S and C377F, are predicted to affect protein folding and maturation. (3) Mutations in the ECD, all of which affect norrin binding, lead to reduced Norrin/β-catenin activation. Notably, M105V and M157V were previously reported not to affect norrin binding, which differs from our findings.[44] We posit that this disparity may stem from differing detection methods, as our employment of Co-IP and immunofluorescence staining methods offers heightened sensitivity. (4)

Investigative Ophthalmology & Visual Science

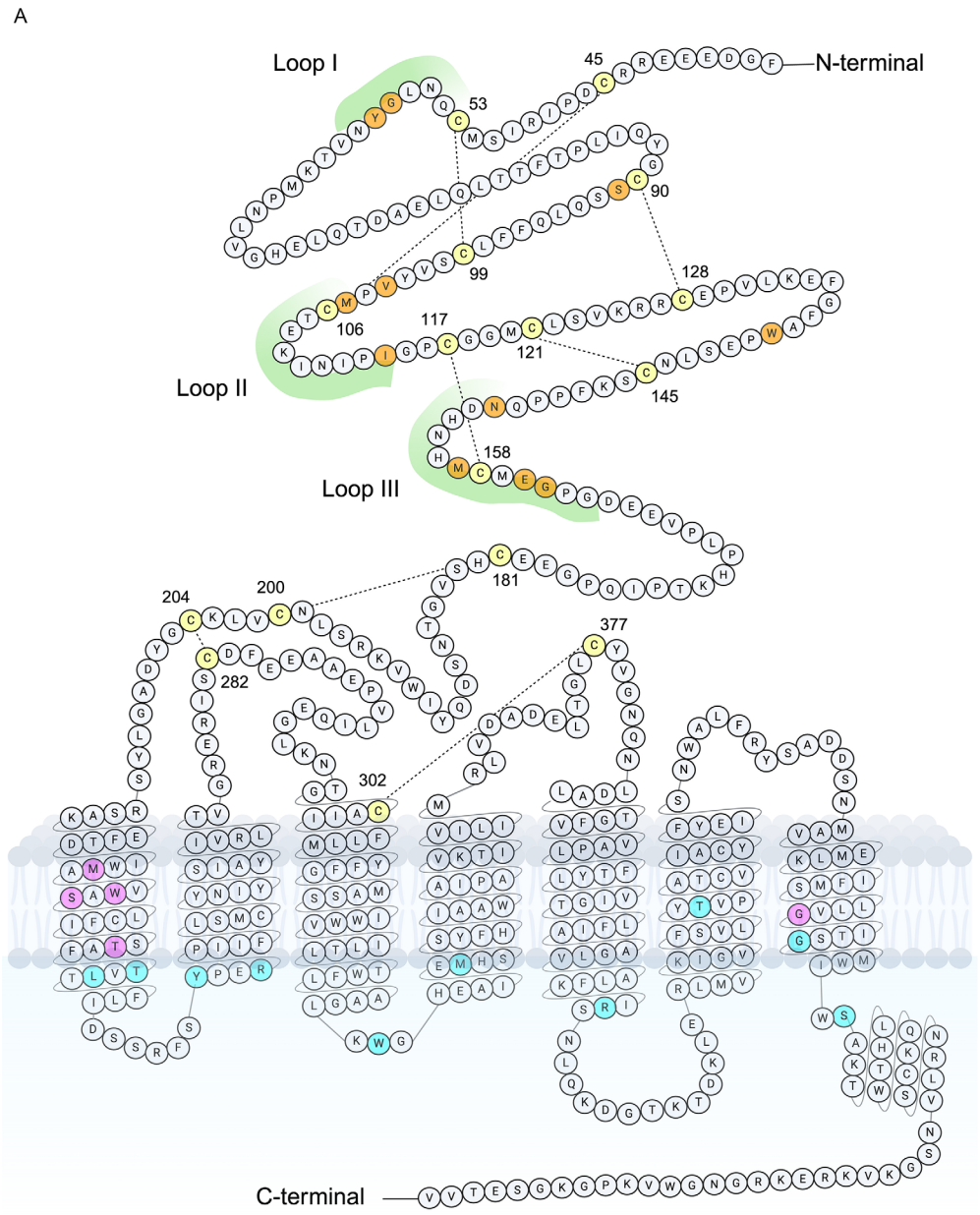

Figure 6. Schematic of the full-length amino acid sequence of FZD4 (excluding the signal peptide, showing amino acids 37–537). Three loops in contact with norrin are denoted in *green*. Cysteine residues involved in the formation of intramolecular disulfide bonds are denoted in *yellow*. Mutation sites affecting norrin binding are denoted in orange, those affecting the membrane localization of FZD4 are denoted in *magenta*, and those affecting the recruitment of DVL2 are denoted in *light blue*.

The majority of mutations located in TM1 and the 488 position in TM7 of FZD4 affect membrane localization. While one previous study found that M105V and M105T in the ECD also affect membrane localization,[29] we observed that M105V could localize normally, consistent with the earlier study by Xu et al.[44] (5) Mutations in the intracellular domain affect DVL2 recruitment. Previous reports have highlighted the extensive influence of the intracellular domain of FZD5 on DVL2 recruitment,[39] and our study corroborates that this finding also applies to FZD4.

For the future functional analysis of newly discovered *FZD4* mutations, we devised the following analytical workflow: Mutants are first constructed on the expression vectors. Validation is performed to ascertain the effect on RNA and protein expression. Then, membrane localization is assessed through immunofluorescence staining. For mutations in the ECD region, the focus is on the norrin-binding capability, which can be evaluated via Co-IP or immunofluorescence staining methods. In the case of mutations in the intracellular domain region, priority is given to the analysis of DVL2 recruitment ability using immunofluorescence staining.

Conclusively, we propose that all *FZD4* missense mutations in FEVR can be classified into five categories based on different functional changes, presenting a domain-based map with detailed functional annotations of various FZD4 missense m*utations*. This map will provide assistance for prenatal counseling and molecular diagnosis for FEVR-associated patients with *FZD4* mutations. Furthermore, this

Investigative Ophthalmology & Visual Science

study provides molecular basis for the development of potential therapeutic approaches for not only FEVR but also other vascular diseases by targeting different domains of FZD4.

The study's limitation lies in the fact that although all analyses are focused on missense mutations, a considerable portion of the mutations include frameshift, nonsense, insertion, deletion, CNV, and splicing.[45] The workflow outlined above may not be suitable for CNV and splicing mutations. Additionally, when dealing with frameshift, nonsense, insertion, and deletion mutations, the challenge arises in classifying alterations involving large segments of amino acids.

Acknowledgments

Supported by the National Natural Science Foundation of China (82371070 to P.Z., 82121003, 82330030 to Z.Y. and 82101153 to M.Y.), the Sichuan Science and Technology program (2023NSFSC0036, 2022ZYD0059, 2023YFS0038 to M.Y., and 2023YFS0119 to Y.H.), the China Postdoctoral Science Foundation (2023M740518 to Y.H.), the Fundamental Research Funds for the Central Universities of Ministry of Education of China (ZYGX2022J023 to S.L.) and the Research Fund of Sichuan Academy of Medical Sciences and Sichuan Provincial People's Hospital (2023BH09 to R.Z. and 2022BH022 to Y.H.). Shanghai Science and Technology Committee (22015820200 to P.Z.).

Disclosure: **E. Dai,** None; **M. Liu,** None; **S. Li,** None; **X. Zhang,** None; **S. Wang,** None; **R. Zhao,** None; **Y. He,** None; **L. Peng,** None; **L. Lv,** None; **H. Xiao,** None; **M. Yang,** None; **Z. Yang,** None; **P. Zhao,** None

References

1. Criswick VG, Schepens CL. Familial exudative vitreoretinopathy. *Am J Ophthalmol*. 1969;68:578–594.
2. Gilmour DF. Familial exudative vitreoretinopathy and related retinopathies. *Eye (Lond)*. 2015;29:1–14.
3. Xu N, Cai Y, Li J, et al. An SNX31 variant underlies dominant familial exudative vitreoretinopathy-like pathogenesis. *JCI insight*. 2023;8(10):e167032.
4. Li S, Yang M, Zhao R, et al. Defective EMC1 drives abnormal retinal angiogenesis via Wnt/beta-catenin signaling and may be associated with the pathogenesis of familial exudative vitreoretinopathy. *Genes Dis*. 2023;10:2572–2585.
5. Yang M, Li S, Huang L, et al. CTNND1 variants cause familial exudative vitreoretinopathy through the Wnt/cadherin axis. *JCI Insight*. 2022;7(14):e158428.
6. Li S, Yang M, He Y, et al. Variants in the Wnt co-receptor LRP6 are associated with familial exudative vitreoretinopathy. *J Genet Genomics*. 2022;49:590–594.
7. Zhu X, Yang M, Zhao P, et al. Catenin alpha 1 mutations cause familial exudative vitreoretinopathy by overactivating Norrin/beta-catenin signaling. *J Clin Invest*. 2021;131(6):e139869.
8. Zhang S, Li X, Liu W, et al. Whole-exome sequencing identified DLG1 as a candidate gene for familial exudative vitreoretinopathy. *Genet Test Mol Biomarkers*. 2021;25:309–316.
9. Zhang L, Zhang X, Xu H, et al. Exome sequencing revealed Notch ligand JAG1 as a novel candidate gene for familial exudative vitreoretinopathy. *Genet Med*. 2020;22:77–84.
10. Park H, Yamamoto H, Mohn L, et al. Integrin-linked kinase controls retinal angiogenesis and is linked to Wnt signaling and exudative vitreoretinopathy. *Nat Commun*. 2019;10:5243.
11. Dixon MW, Stem MS, Schuette JL, Keegan CE, Besirli CG. CTNNB1 mutation associated with familial exudative vitreoretinopathy (FEVR) phenotype. *Ophthalmic Genet*. 2016;37:468–470.
12. Mears K, Bakall B, Harney LA, Penticoff JA, Stone EM. Autosomal dominant microcephaly associated with congenital lymphedema and chorioretinopathy due to a novel mutation in KIF11. *JAMA Ophthalmol*. 2015;133:720–721.
13. Collin RW, Nikopoulos K, Dona M, et al. ZNF408 is mutated in familial exudative vitreoretinopathy and is crucial for the development of zebrafish retinal vasculature. *Proc Natl Acad Sci USA*. 2013;110:9856–9861.
14. Khan K, Logan CV, McKibbin M, et al. Next generation sequencing identifies mutations in Atonal homolog 7 (ATOH7) in families with global eye developmental defects. *Hum Mol Genet*. 2012;21:776–783.
15. Junge HJ, Yang S, Burton JB, et al. TSPAN12 regulates retinal vascular development by promoting Norrin- but not Wnt-induced FZD4/beta-catenin signaling. *Cell*. 2009;139:299–311.
16. Toomes C, Bottomley HM, Jackson RM, et al. Mutations in LRP5 or FZD4 underlie the common familial exudative vitreoretinopathy locus on chromosome 11q. *Am J Hum Genet*. 2004;74:721–730.
17. Jiao X, Ventruto V, Trese MT, Shastry BS, Hejtmancik JF. Autosomal recessive familial exudative vitreoretinopathy is associated with mutations in LRP5. *Am J Hum Genet*. 2004;75:878–884.
18. Downey LM, Keen TJ, Roberts E, Mansfield DC, Bamashmus M, Inglehearn CF. A new locus for autosomal dominant familial exudative vitreoretinopathy maps to chromosome 11p12-13. *Am J Hum Genet*. 2001;68:778–781.
19. Chen ZY, Battinelli EM, Fielder A, et al. A mutation in the Norrie disease gene (NDP) associated with X-linked familial exudative vitreoretinopathy. *Nat Genet*. 1993;5:180–183.
20. Salvo J, Lyubasyuk V, Xu M, et al. Next-generation sequencing and novel variant determination in a cohort of 92 familial exudative vitreoretinopathy patients. *Invest Ophthalmol Vis Sci*. 2015;56:1937–1946.
21. Li JK, Li Y, Zhang X, et al. Spectrum of variants in 389 Chinese probands with familial exudative vitreoretinopathy. *Invest Ophthalmol Vis Sci*. 2018;59:5368–5381.
22. Schulte G, Bryja V. The Frizzled family of unconventional G-protein-coupled receptors. *Trends Pharmacol Sci*. 2007;28:518–525.
23. Zhou Y, Wang Y, Tischfield M, et al. Canonical WNT signaling components in vascular development and barrier formation. *J Clin Invest*. 2014;124:3825–3846.
24. Robitaille J, MacDonald ML, Kaykas A, et al. Mutant frizzled-4 disrupts retinal angiogenesis in familial exudative vitreoretinopathy. *Nat Genet*. 2002;32:326–330.
25. Lu J, Huang L, Sun L, et al. FZD4 in a large Chinese population with familial exudative vitreoretinopathy: molecular characteristics and clinical manifestations. *Invest Ophthalmol Vis Sci*. 2022;63:7.
26. Smallwood PM, Williams J, Xu Q, Leahy DJ, Nathans J. Mutational analysis of Norrin-Frizzled4 recognition. *J Biol Chem*. 2007;282:4057–4068.
27. Zhang K, Harada Y, Wei X, et al. An essential role of the cysteine-rich domain of FZD4 in Norrin/Wnt signaling and familial exudative vitreoretinopathy. *J Biol Chem*. 2011;286:10210–10215.
28. Han S, Sun J, Yang L, Qi M. Role of NDP- and FZD4-related novel mutations identified in patients with FEVR in Norrin/beta-catenin signaling pathway. *BioMed Res Int*. 2020;2020:7681926.
29. Milhem RM, Ben-Salem S, Al-Gazali L, Ali BR. Identification of the cellular mechanisms that modulate trafficking of frizzled family receptor 4 (FZD4) missense mutants associated with familial exudative vitreoretinopathy. *Invest Ophthalmol Vis Sci*. 2014;55:3423–3431.

Investigative Ophthalmology & Visual Science

30. Pau MS, Gao S, Malbon CC, Wang HY, Bertalovitz AC. The intracellular loop 2 F328S frizzled-4 mutation implicated in familial exudative vitreoretinopathy impairs dishevelled recruitment. *J Mol Signal*. 2015;10:5.
31. Strakova K, Matricon P, Yokota C, et al. The tyrosine Y250(2.39) in Frizzled 4 defines a conserved motif important for structural integrity of the receptor and recruitment of Disheveled. *Cell Signal*. 2017;38:85–96.
32. Kashani AH, Brown KT, Chang E, Drenser KA, Capone A, Trese MT. Diversity of retinal vascular anomalies in patients with familial exudative vitreoretinopathy. *Ophthalmology*. 2014;121:2220–2227.
33. Kashani AH, Learned D, Nudleman E, Drenser KA, Capone A, Trese MT. High prevalence of peripheral retinal vascular anomalies in family members of patients with familial exudative vitreoretinopathy. *Ophthalmology*. 2014;121:262–268.
34. Wang S, Zhang X, Hu Y, et al. Clinical and genetical features of probands and affected family members with familial exudative vitreoretinopathy in a large Chinese cohort. *Br J Ophthalmol*. 2021;105:83–86.
35. Chang TH, Hsieh FL, Zebisch M, Harlos K, Elegheert J, Jones EY. Structure and functional properties of Norrin mimic Wnt for signalling with Frizzled4, Lrp5/6, and proteoglycan. *eLife*. 2015;4:e06554.
36. Yang S, Wu Y, Xu TH, et al. Crystal structure of the Frizzled 4 receptor in a ligand-free state. *Nature*. 2018;560:666–670.
37. Vagin O, Kraut JA, Sachs G. Role of N-glycosylation in trafficking of apical membrane proteins in epithelia. *Am J Physiol Renal Physiol*. 2009;296:F459–F469.
38. Tauriello DV, Jordens I, Kirchner K, et al. Wnt/beta-catenin signaling requires interaction of the Dishevelled DEP domain and C terminus with a discontinuous motif in Frizzled. *Proc Natl Acad Sci USA*. 2012;109:E812–E820.
39. Gammons MV, Renko M, Johnson CM, Rutherford TJ, Bienz M. Wnt signalosome assembly by DEP Domain Swapping of Dishevelled. *Mol Cell*. 2016;64:92–104.
40. Bang I, Kim HR, Beaven AH, et al. Biophysical and functional characterization of Norrin signaling through Frizzled4. *Proc Natl Acad Sci USA*. 2018;115:8787–8792.
41. Tao T, Xu N, Li J, et al. Ocular features and mutation spectrum of patients with familial exudative vitreoretinopathy. *Invest Ophthalmol Vis Sci*. 2021;62:4.
42. Valnohova J, Kowalski-Jahn M, Sunahara RK, Schulte G. Functional dissection of the N-terminal extracellular domains of Frizzled 6 reveals their roles for receptor localization and Dishevelled recruitment. *J Biol Chem*. 2018;293:17875–17887.
43. Dailey WA, Gryc W, Garg PG, Drenser KA. Frizzled-4 variations associated with retinopathy and intrauterine growth retardation: a potential marker for prematurity and retinopathy. *Ophthalmology*. 2015;122:1917–1923.
44. Xu Q, Wang Y, Dabdoub A, et al. Vascular development in the retina and inner ear: control by Norrin and Frizzled-4, a high-affinity ligand-receptor pair. *Cell*. 2004;116:883–895.
45. Xiao H, Tong Y, Zhu Y, Peng M. Familial exudative vitreoretinopathy-related disease-causing genes and Norrin/β-catenin signal pathway: structure, function, and mutation spectrums. *J Ophthalmol*. 2019;2019:5782536.
46. Richards S, Aziz N, Bale S, et al. Standards and guidelines for the interpretation of sequence variants: a joint consensus recommendation of the American College of Medical Genetics and Genomics and the Association for Molecular Pathology. *Genet Med*. 2015;17:405–424.
47. Cicerone AP, Dailey W, Sun M, et al. A survey of multigenic protein-altering variant frequency in familial exudative vitreo-retinopathy (FEVR) patients by targeted sequencing of seven FEVR-linked genes. *Genes*. 2022;13(3):495.
48. Jia LY, Li XX, Yu WZ, Zeng WT, Liang C. Novel frizzled-4 gene mutations in chinese patients with familial exudative vitreoretinopathy. *Arch Ophthalmol*. 2010;128:1341–1349.
49. Toomes C, Bottomley HM, Scott S, et al. Spectrum and frequency of FZD4 mutations in familial exudative vitreoretinopathy. *Invest Ophthalmol Vis Sci*. 2004;45:2083–2090.
50. Nikopoulos K, Venselaar H, Collin RW, et al. Overview of the mutation spectrum in familial exudative vitreoretinopathy and Norrie disease with identification of 21 novel variants in FZD4, LRP5, and NDP. *Hum Mutat*. 2010;31:656–666.
51. Tang M, Ding X, Li J, et al. Novel mutations in FZD4 and phenotype-genotype correlation in Chinese patients with familial exudative vitreoretinopathy. *Mol Vis*. 2016;22:917–932.
52. Chen C, Sun L, Li S, et al. The spectrum of genetic mutations in patients with asymptomatic mild familial exudative vitreoretinopathy. *Exp Eye Res*. 2020;192:107941.
53. Zhu X, Sun K, Huang L, et al. Identification of novel mutations in the FZD4 and NDP genes in patients with familial exudative vitreoretinopathy in South India. *Genet Test Mol Biomarkers*. 2020;24:92–98.
54. Robitaille JM, Zheng B, Wallace K, et al. The role of Frizzled-4 mutations in familial exudative vitreoretinopathy and Coats disease. *Br J Ophthalmol*. 2011;95:574–579.
55. Robitaille JM, Wallace K, Zheng B, et al. Phenotypic overlap of familial exudative vitreoretinopathy (FEVR) with persistent fetal vasculature (PFV) caused by FZD4 mutations in two distinct pedigrees. *Ophthalmic Genet*. 2009;30:23–30.
56. Musada GR, Syed H, Jalali S, Chakrabarti S, Kaur I. Mutation spectrum of the FZD-4, TSPAN12 AND ZNF408 genes in Indian FEVR patients. *BMC Ophthalmol*. 2016;16:90.
57. Xu H, Zhang S, Huang L, et al. Identification of novel variants in the FZD4 gene associated with familial exudative vitreoretinopathy in Chinese families. *Clin Exp Ophthalmol*. 2020;48:356–365.
58. Wang Z, Chen C, Sun L, et al. Symmetry of folds in FEVR: a genotype-phenotype correlation study. *Exp Eye Res*. 2019;186:107720.
59. Mao J, Chen Y, Fang Y, et al. Clinical characteristics and mutation spectrum in 33 Chinese families with familial exudative vitreoretinopathy. *Ann Med*. 2022;54:3286–3298.
60. Seo SH, Yu YS, Park SW, et al. Molecular characterization of FZD4, LRP5, and TSPAN12 in familial exudative vitreoretinopathy. *Invest Ophthalmol Vis Sci*. 2015;56:5143–5151.
61. Iarossi G, Bertelli M, Maltese PE, et al. Genotype-phenotype characterization of novel variants in six Italian patients with familial exudative vitreoretinopathy. *J Ophthalmol*. 2017;2017:3080245.
62. Yang H, Li S, Xiao X, Wang P, Guo X, Zhang Q. Identification of FZD4 and LRP5 mutations in 11 of 49 families with familial exudative vitreoretinopathy. *Mol Vis*. 2012;18:2438–2446.
63. Boonstra FN, van Nouhuys CE, Schuil J, et al. Clinical and molecular evaluation of probands and family members with familial exudative vitreoretinopathy. *Invest Ophthalmol Vis Sci*. 2009;50:4379–4385.
64. Tian T, Chen C, Zhang X, Zhang Q, Zhao P. Clinical and genetic features of familial exudative vitreoretinopathy with only-unilateral abnormalities in a Chinese cohort. *JAMA Ophthalmol*. 2019;137:1054–1058.
65. Chen C, Wang Z, Sun L, et al. Next-generation sequencing in the familial exudative vitreoretinopathy-associated rhegmatogenous retinal detachment. *Invest Ophthalmol Vis Sci*. 2019;60:2659–2666.
66. Yang L, Fu J, Cheng J, et al. A novel variant of the FZD4 gene in a chinese family causes autosomal dominant

Investigative Ophthalmology & Visual Science

familial exudative vitreoretinopathy. *Cell Physiol Biochem*. 2018;51:2445–2455.

67. Bochicchio S, Pellegrini M, Cereda M, Oldani M, Staurenghi G. Macular hole in a young patient affected by familial exudative vitreoretinopathy. *Retin Cases Brief Rep*. 2020;14:6–9.
68. Qu N, Li W, Han DM, et al. Mutation spectrum in a cohort with familial exudative vitreoretinopathy. *Mol Genet Genomic Med*. 2022;10:e2021.
69. Tian T, Zhang X, Zhang Q, Zhao P. Variable reduction in Norrin signaling activity caused by novel mutations in FZD4 identified in patients with familial exudative vitreoretinopathy. *Mol Vis*. 2019;25:60–69.
70. Carrera W, Ng C, Desler C, Jumper JM, Agarwal A. Novel FZD4 and LRP5 mutations in a small cohort of patients with familial exudative vitreoretinopathy (FEVR). *Ophthalmic Genet*. 2021;42:200–203.
71. Yoshida S, Arita R, Yoshida A, et al. Novel mutation in FZD4 gene in a Japanese pedigree with familial exudative vitreoretinopathy. *Am J Ophthalmol*. 2004;138:670–671.
72. Dan H, Wang D, Huang Z, et al. Whole exome sequencing revealed 14 variants in NDP, FZD4, LRP5, and TSPAN12 genes for 20 families with familial exudative vitreoretinopathy. *BMC Med Genomics*. 2022;15:54.
73. Qin M, Kondo H, Tahira T, Hayashi K. Moderate reduction of Norrin signaling activity associated with the causative missense mutations identified in patients with familial exudative vitreoretinopathy. *Hum Genet*. 2008;122:615–623.

Investigative Ophthalmology & Visual Science